Australian Government
Department of Defence
Defence Science and
Technology Organisation

An Investigation into Performance Modelling of a Small Gas Turbine Engine

Zafer Leylek

Air Vehicles Division
Defence Science and Technology Organisation

DSTO-TR-2757

ABSTRACT

A small gas turbine performance modelling and testing project has been completed as part of a Divisional Enabling Research Program (DERP). The main objective of the program was to enhance DSTO's capability in understanding and modelling the thermodynamic and performance characteristics of gas turbine engines. Secondary objectives of the program included the investigation of thrust augmentation technologies and infrared suppression modelling and analysis. This report presents the results of both numerical and experimental investigation into engine performance simulation. It outlines the different tools and techniques used in modeling engine component behaviour and discusses their advantages and disadvantages. The results of two different tests designed to explore engine operating regions close to compressor stall and surge is presented.

Published by

Air Vehicles Division
DSTO Defence Science and Technology Organisation
506 Lorimer St
Fishermans Bend, Victoria 3207 Australia

Telephone: (03) 9626 7000
Fax: (03) 9626 7999

AR-015-427
October 2012

APPROVED FOR PUBLIC RELEASE

An Investigation into Performance Modelling of a Small Gas Turbine Engine

Executive Summary

A small gas turbine performance modelling and testing project has been completed as part of a Divisional Enabling Research Program (DERP). The main objective of the program was to enhance DSTO's capability in understanding and modelling the thermodynamic and performance characteristics of gas turbine engines. Secondary objectives of the program included the investigation of thrust augmentation technologies and infrared suppression modelling and analysis.

Engine performance modelling was conducted using commercial software and an in-house developed code. The engine performance model of the small gas turbine engine was validated through engine testing. A number of non-standard tests were also conducted in order to "stress" the engine and compare results with the engine performance model and to provide an insight into thrust augmentation options. A number of auxilary tools and techniques were developed during this process.

The primary objectives of the project were successfully reached. An engine performance modelling tool was developed and validated and different tools and techniques were evaluated. Infrared suppression related studies were also conducted.

A number of other projects have been initiated based on the tools, technologies and processes developed during this project. An alternate fuels research program will directly utilise the testing infrastructure, tools and know-how. A PhD into infrared prediction technologies is currently under way and a final year thesis completed. A feasibility study into compressor and turbine performance testing will be completed. A number of numerical tools will continue to be developed to aid and improve the modelling of engine performance components.

The tools, techniques and conclusions derived from this project have direct impact on Australian Defence Organisation outcomes. Engine performance modelling is critical for ADF gas turbine engine performance analysis and requirements, structural, thermal and creep assessment, performance degradation studies, infrared suppression technologies to name a few. The tools and techniques developed in this project will be directly used to model the performance of ADF gas turbine engines.

Author

Zafer Leylek
Air Vehicles Division

Zafer Leylek has worked in the Infrared Signatures and Aerothermodynamics group of the Defence Science and Technology Organisation since 2010. He completed his undergraduate training at the Royal Melbourne Institute of Technology (RMIT), in Aerospace Engineering and a graduate certificate degree in Computer Systems Engineering. Zafer has over ten years experience in engine performance and aerodynamic design and has worked on a large scale European engine development program.

Contents

NOMENCLATURE

b = Combustor part load constant
f = Fuel to mass flow ratio or scale factor
h = Enthalpy
F = Force
P = Pressure
T = Temperature
W = Mass flow rate
V = Volume
π = total-total pressure ratio
η = total-total efficiency
Ω = Combustor/burner loading

Subscripts

t = total thermodynamic conditions
ref = reference
des = design
ds = design speed
D = discharge
FG = gross thrust
N = net
0 = atmospheric conditions
1 = compressor inlet
2 = compressor outlet/combustor inlet
3 = combustor outlet/turbine inlet
4 = turbine outlet/exhaust inlet
6 = exhaust outlet/nozzle inlet
8 = nozzle exit

Superscripts

‘ = relative value in the rotating coordinate system

ACRONYMS

rpm = Revolutions per Minute
CFD = Computational Fluid Dynamics
CORR = Corrected
DERP = Divisional Enabling Research Program
DP = Design Point
DP (MAP) = Component Map Design Point
EGT = Exhaust Gas Temperature
HPC = High Pressure Compressor
HPT = High Pressure Turbine
RNI = Reynolds Number Index
OL = Operating Line

1. Introduction

A small gas turbine performance modelling and testing project has been completed as part of a Divisional Enabling Research Program (DERP). The main objective of the program was to enhance DSTO's capability in understanding and modelling the thermodynamic and performance characteristics of gas turbine engines. A small gas turbine engine was chosen to reduce the cost and time associated with testing larger engines. As part of this objective DSTO's small engine test capabilities were enhanced and an extensive testing and validation program completed.

Secondary objectives of the program were to: investigate thrust augmentation options; undertake modelling and analyses of infrared suppression technologies; provide a foundation and test bed for future alternate fuels research; and initiate co-operative research programs with universities.

Numerical modelling of engine performance and thermodynamics involved:

- engine disassembly,
- component geometry scanning,
- compressor and turbine mean-line and through flow analyses using TurbAero[1] and CompAero[2],
- computational fluid dynamics modelling of the compressor and turbine using Numeca[3], and
- development of a turbojet engine performance simulation code to enhance the capabilities of Gasturb[4].

Testing and validation included:

- designing and constructing a small gas turbine engine performance test bed,
- designing and constructing a bell-mouth,
- instrumentation analysis and installation,
- data acquisition, and
- engine component modifications and installations.

2. AMT Olympus HP Turbojet

The AMT Olympus HP turbojet engine was used as the benchmark engine. Figure 1 shows the AMT Olympus HP engine.

Figure 1 Olympus HP Gas Turbine Engine

The Olympus HP gas turbine engine is a single spool turbojet engine. It is comprised of a standard inlet, single stage centrifugal compressor with vaned diffusers, annular combustor, single stage axial turbine and convergent nozzle. The engine is controlled using an Engine Control Unit (ECU) and comes with an electric starter motor.

The main engine performance characteristics provided by the engine manufacturer can be seen in Table 1.

Table 1 Olympus HP engine performance parameters[5,6]

Parameter	**Condition (ISA, SLS)**	**Value**
Thrust	108000 rpm	230 N
Pressure Ratio	108000 rpm	4
Mass Flow Rate	108000 rpm	450 g/sec
Maximum Speed		108000 rpm
Maximum Allowed Speed		112000 rpm
Exhaust Temperature		700^0 C
Maximum Exhaust Temperature		750^0 C
Fuel usage	108000 rpm	640 g/min
Fuel type		Kerosene/paraffin/A-1/white spirit

The electric starter motor was removed and replaced with an air starter system. The reasons for removing the electric starter were to ensure uniform flow through the bell-mouth for mass flow rate measurement, eliminate a source of loss and turbulence to the engine compressor and provide a standard configuration for all tests.

A three stage process is used to start the engine. The first stage requires shop compressed air to be directed onto the impeller through a slot in the intake to bring rotation up to 9000 rpm. After this, propane is pumped into the combustor to initiate combustion. Then, once the engine speed reaches approximately 50,000 rpm, the propane gas valve is shut-off and replaced with kerosene. Thereafter the engine can be operated normally.

3. Engine Numerical Modelling

The engine performance and thermodynamic cycle is simulated using a combination of commercial and in-house engine performance codes, empirical based component analysis tools and CFD. Figure 2 shows a breakdown of the engine components and the tools used in predicting thermodynamic behaviour.

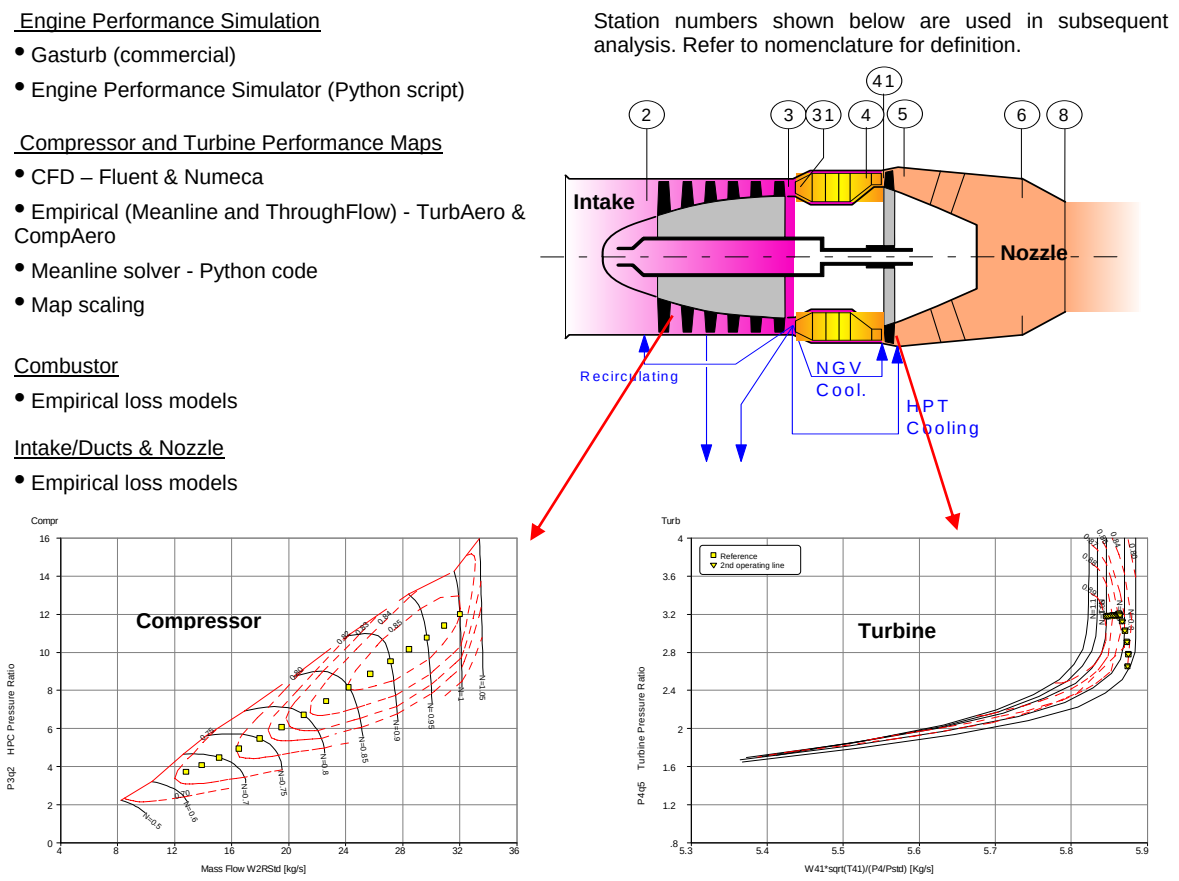

Figure 2 Engine and component performance models and tools used to predict their behaviour

3.1 System Performance Modelling

The performance of each component is combined in an engine performance model. A commercial code, Gasturb[4], was used as the main performance simulator. In order to enhance and adapt various models to the Olympus HP engine an in-house engine performance code was developed. This code was subsequently validated with Gasturb.

The component performance models are combined to produce a system of non-linear equations with the engine performance code. For a simple turbojet configuration the system is solved using the following relationships:

Mechanical coupling: $N_{HPC} = N_{HPT}$

Energy balance between HPC & HPT: $h_{T3} - h_{T2} = \eta_m (1+f)(h_{T4} - h_{T5})$

Mass flow balance: $W_{HPC}(1+f) = W_{HPT}$

3.2 Intake

The intake is modelled as an adiabatic system. The intake loss is primarily correlated with the inlet corrected flow rate or Mach number. In this instance, the dependency is expressed using the intake inlet and outlet total pressure ratio.

The intake pressure loss ratio was assumed to be constant for the Olympus HP intake. This assumption was made after considering a) the sensitivity of the intake loss model accuracy on overall system performance, b) instrumentation constraints and uncertainties in a comprehensive intake test, c) the lack of resources needed for testing and d) a literature survey. Test results subsequently showed this assumption to be valid.

The equation set used in the engine performance calculations for the intake are:

$$\pi_{\text{int } ake} = \frac{P_{t2}}{P_{t0}} = const = 0.98$$

$$h_{t0} = h_{t2}$$

3.3 Compressor

The Olympus HP compressor consists of an impeller, radial vaned diffuser and axial guide vanes. The impeller has seven blades and seven splitter vanes. The radial diffuser contains fifteen vanes followed by thirty axial guide vanes.

The compressor is arguably the most challenging component for thermodynamic performance prediction. A number of different approaches to generating performance curves were evaluated with limited success. The techniques used to generate compressor performance curves included CFD modelling, mean-line and through-flow modelling, literature and map scaling.

3.3.1 Map Scaling

Map scaling is a commonly used technique where published performance maps of compressors with the same configuration and capacity are scaled using known reference points or curves. The reference point at which maps are usually scaled is the compressor

design point. Assuming that the Olympus HP compressor design point is known or can be inferred from existing performance data, the equations used to scale the corrected mass flow rate, efficiency and pressure ratio can be written as:

$$f_{mass} = \frac{W_{CORR,DP}}{W_{CORR,DP(MAP)} * f_{W,RNI}}$$

$$f_{\eta} = \frac{\eta_{DP}}{\eta_{DP(MAP)} * f_{\eta,RNI}}$$

$$f_{P_3/P_2} = \frac{(P_3/P_2)_{DP} - 1}{(P_3/P_2)_{DP(MAP)-1}}$$

$$f_N = \frac{N_{DP}}{N_{DP(MAP)}}$$

$$RNI = \frac{P_t}{P_{t,ref}} \sqrt{\frac{R_{ref} T_{t,ref}}{R T_t}} \frac{\mu_{ref}}{\mu}$$

$$f_{W,RNI} = \begin{cases} 0.022 \ln(RNI) + 1 & \ln(RNI) < 0 \\ 1 & \ln(RNI) \geq 0 \end{cases}$$

$$f_{\eta,RNI} = \begin{cases} 0.011 \ln(RNI) + 1 & \ln(RNI) < 0 \\ 1 & \ln(RNI) \geq 0 \end{cases}$$

Where *f* is the scaling factor and RNI is the Reynolds Number Index.

Figure 3 illustrates the map scaling process graphically.

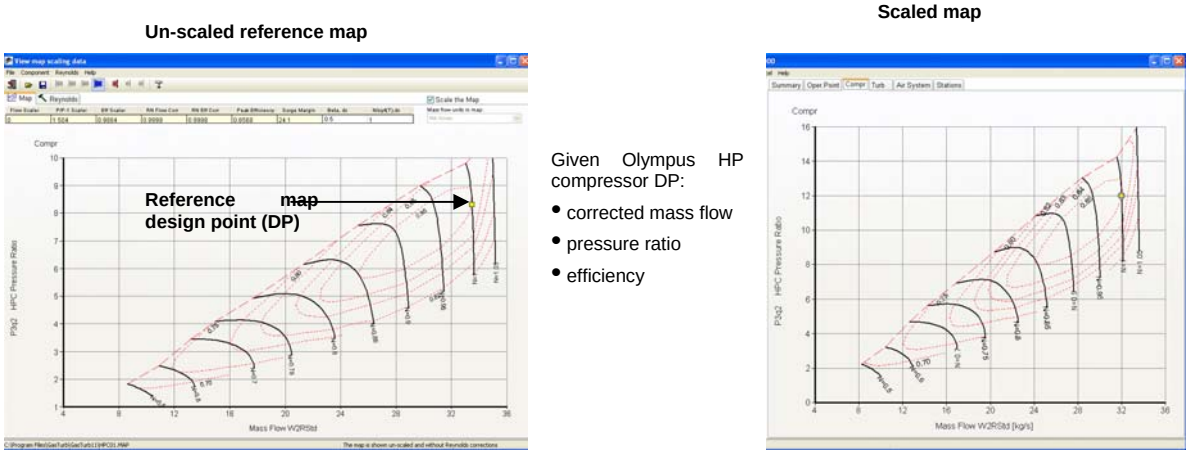

Figure 3 Map scaling process

The standard map scaling process is better suited for gas turbine design applications where the design point data of the new engine is known. Also the map scaling point only has a single control lever, namely the scaling factor.

This technique has been modified for performance modelling of existing engines where separate scaling factors are applied to each speed line to better approximate measured test data. This results in a set of map scaling parameters and allows the reference map to also be shifted and/or skewed for each speed line.

The reference map used to scale and construct the Olympus HP map belongs to the Olympus engine as published in Rahman[7].

The Olympus HP compressor design point is not published by the manufacturer. The pressure ratio and mass flow for the compressor is given at the maximum operating speed. Hence the design point corrected mass flow rate, efficiency and pressure ratio for the compressor has to be estimated. Although this may yield reasonable results, the engine test setup and instrumentation were designed so that the compressor corrected mass flow rate, pressure ratio and efficiency could be estimated at different rotational speeds. This in turn allows the calculation of the compressor operating line which is used to further refine or calibrate the map scaling process, enhancing overall engine performance prediction.

3.3.2 Compressor Performance Map

The Olympus compressor map published by Rahman[7] was used as the baseline map. The compressor map was scaled using the compressor performance parameters measured during the operating line test. Figure 4 shows the unscaled and scaled Olympus compressor map.

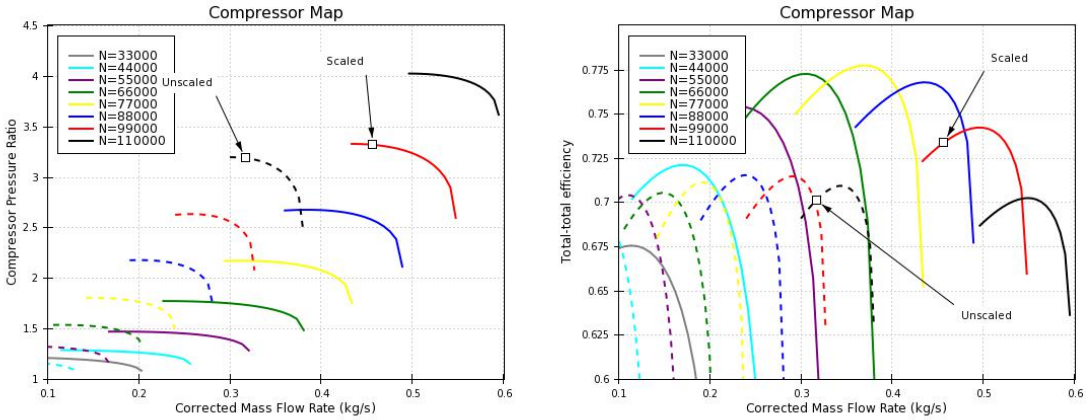

Figure 4 Unscaled and scaled compressor map

3.4 Combustor

The combustor is of an annular type with six fuel nozzles. The design of the combustor is fairly crude and consists of an annular cylinder and six fuel nozzles.

The combustor thermodynamic performance is estimated using common empirical models. Modern day combustion systems exhibit very good performance with very little losses. The application of loss and performance models to a combustor with crude design raises a number of issues and presents added complications. The only way to resolve these complications is to conduct component testing which was deemed too costly in terms of time and money. The test requires specialised expertise and testing equipment and the gain in data was deemed insufficient when considering the overall scope of the project.

Another added complication to the Olympus HP combustor performance prediction is the inclusion of oil in the fuel system. The fuel is pre-mixed with 4.5% Aeroshell 500 turbine oil before use. The fuel line from the tank is split into two with one line leading to the combustor fuel nozzles and the other onto the bearing system. The mechanical design of the shaft/bearing system is such that the fuel/oil mix returns to the combustor once it has passed over the bearings. Hence, the complication is doubled in that not only the effect of the oil on combustion but also the affect of the lubrication fuel/oil returning to the combustor needs to be accounted for.

The combustor efficiency can be correlated with the combustor loading (Gasturb) which is defined as:

$$\Omega = \frac{W_{31}}{P_3^{1.8} e^{T_3/300} V}$$

An empirical loss model has been used to estimate the change in combustor efficiency at off-design conditions. The combustor efficiency at off-design conditions can be calculated as:

$$\log(1-\eta) = \log(1-\eta_{des}) + b * \log\left(\frac{\Omega}{\Omega_{des}}\right)$$

where b = 1.6.

The pressure loss in the combustor is dependent on inlet corrected mass flow rate which is modelled as a duct (see section 3.6 for details).

3.5 Turbine

The Olympus HP turbine contains a single stage axial turbine with 22 Nozzle Guide Vanes (NGV) and 29 rotor blades. The turbine is unshrouded. A picture of the Olympus HP turbine NGV and rotor can be seen in Figure 5.

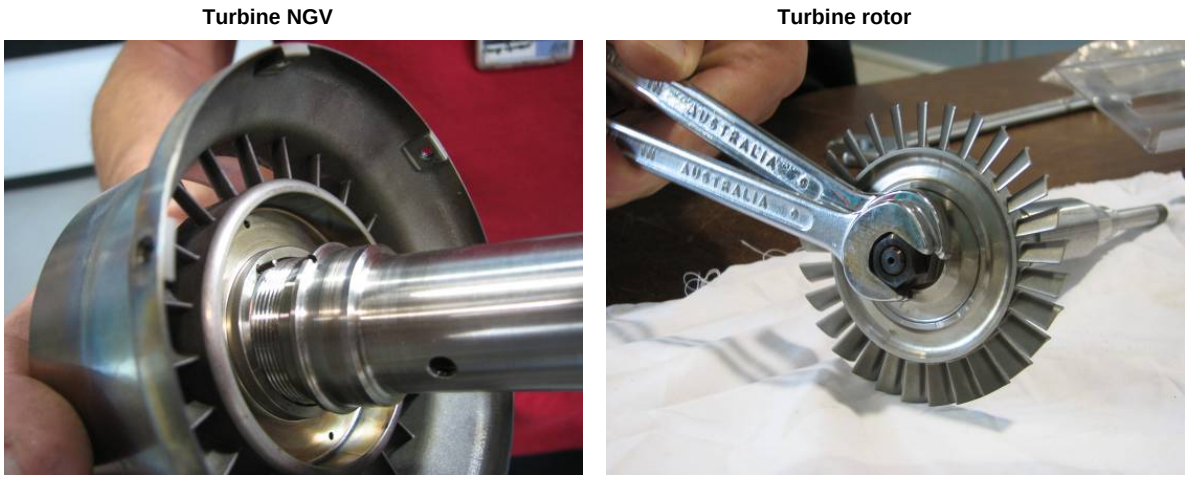

Figure 5 Olympus HP turbine NGV and rotor

Initially two different techniques were used to predict the performance characteristics of the turbine. The first method was based on CFD and the second method the mean-line and through-flow code TurbAero. Subsequent modelling showed that the results needed to be scaled in order to improve correlation between test and model results; hence map scaling has also been applied to obtain the final turbine map.

The main input when conducting CFD modelling and to a lesser extent mean-line and through-flow technique is a detailed knowledge of the geometry. Hence the engine was dismantled and optical scanning was used to generate a geometric point cloud. Figure 6 shows the optical scan results of the turbine nozzle and rotor.

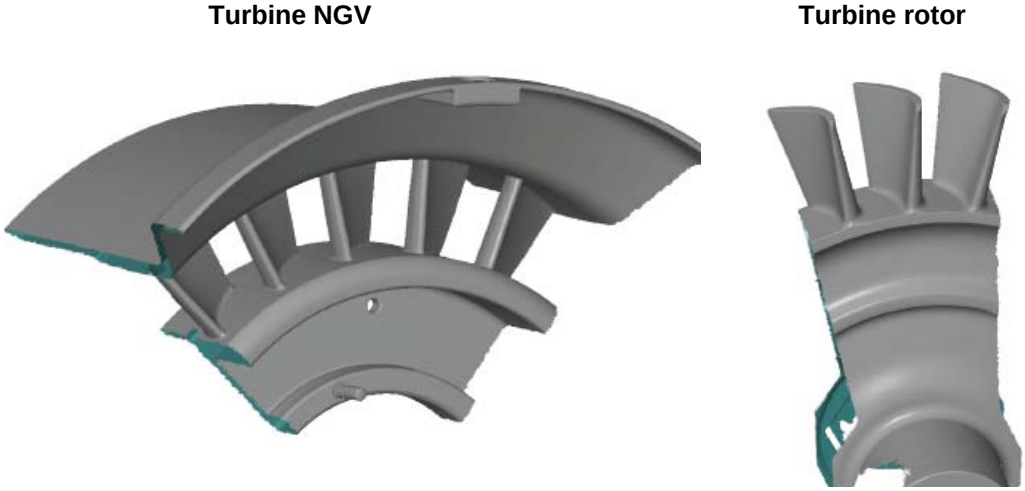

Figure 6 Optical scan plot of the Olympus HP turbine nozzle and rotor

The optical scan yields a very large dataset. The accuracy is dependent on a number of factors including part shape, size, surface finish and a number of optical scanning parameters. The accuracy for the component scan was stated to be below 20-30 micron which was deemed sufficient for modelling purposes.

Although data points generated with optical scanning are highly accurate, kinks are formed in regions where optical visibility and access is poor and complex geometric features are present. Hence, post-processing is required to eliminate these kinks before proceeding to CFD and mean-line and through-flow analysis. Capturing and defining sharp corners is also difficult to achieve with a cloud of geometric data points and so requires special attention and treatment.

A number of blade section profiles were then generated from the post-processed geometric data points using a 3D CAD package. This is required for clean geometry and mesh construction. It is also required to define key blade profile parameters for mean-line and through-flow analysis.

Figure 7 shows the blade and cross section profiles of the turbine nozzle and rotor.

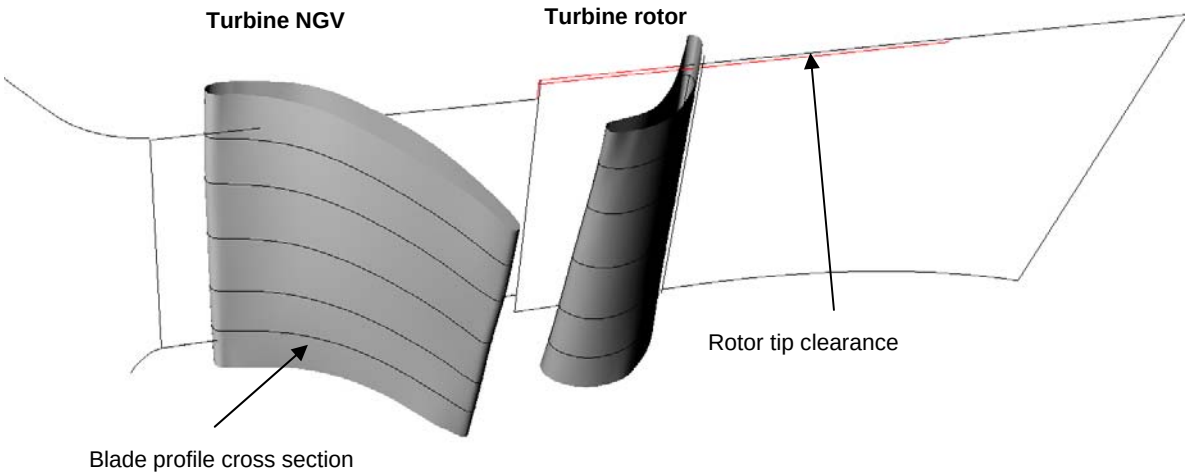

Figure 7 Olympus HP turbine cross section and blade profile plot

Figure 8 shows some of the key blade profile performance parameters measured for mean-line and through-flow analysis.

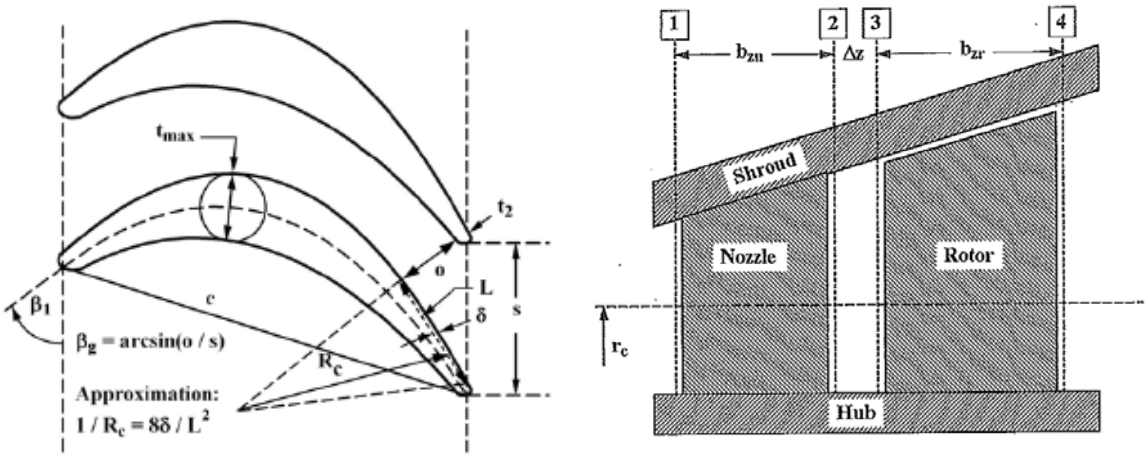

Figure 8 Main blade geometric parameters used in mean-line and through-flow analysis

3.5.1 CFD Modelling

A CFD model of the Olympus HP turbine was constructed and solved using Numeca[3] Fine/TURBO suit of tools. Figure 9 shows the Olympus HP turbine CFD model.

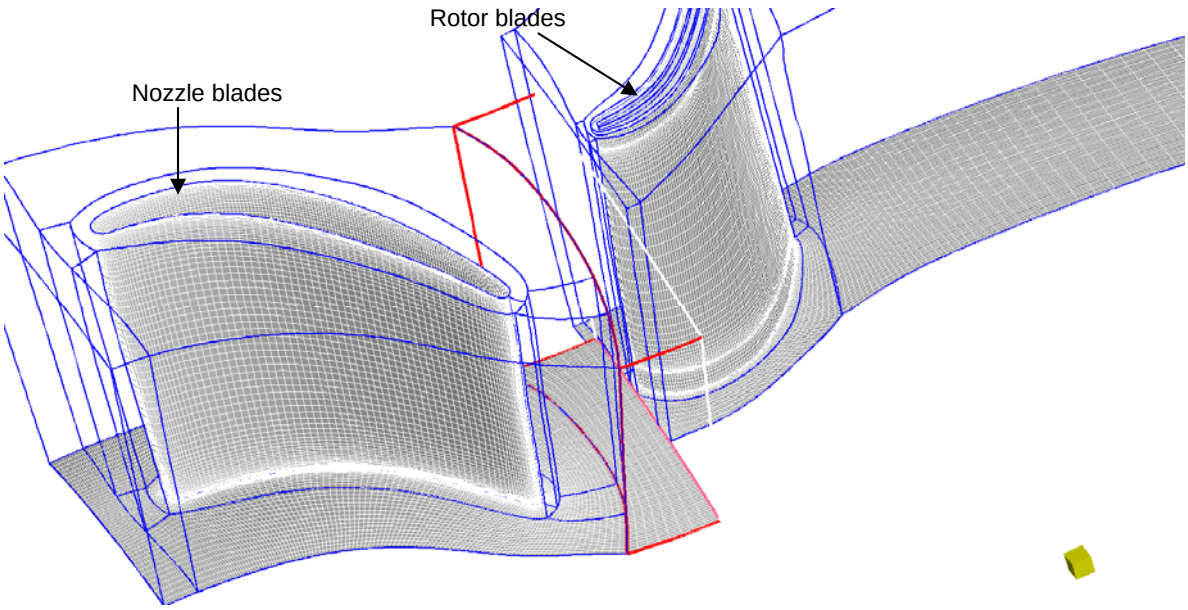

Figure 9 Olympus HP turbine CFD model

The mesh contains approximately two million grid points. The air is modelled as a compressible ideal fluid and specific heats a function of temperature. The solver recommended standard Spalart-Allmaras turbulence model was used during simulations. A standard turbine inlet total temperature of 1000K and 300 kPa total inlet pressure was used as the standard operating condition. The turbine rotational speed was varied from

60K rpm to 110K rpm with 10K rpm increments to obtain 5 speed lines. For each turbine rotational speed 12 different outlet static pressure boundary conditions were applied to simulate performance ranging from slow subsonic to choked flow. Hence, a total of 60 CFD simulations were successfully completed to provide an accurate representation of the turbine performance throughout its operating envelope.

It should be noted that the performance maps are generated in non-dimensionalised form. Flow similarity in a rotating component is dependent on three independent parameters, namely the inlet corrected mass flow rate, corrected rotational speed and Reynolds number. These three parameters can also be expressed in different forms such as Mach number, flow coefficient, loading coefficient etc. The corrected mass flow rate and corrected rotational speed are the two primary parameters that determine the component performance. It has been shown that Reynolds numbers above 100,000 do not alter rotating component performance and Reynolds number effects are negligible. Since the CFD based map generation approach ensures that the corrected flow rate and speeds are matched, the error introduced by the arbitrary selection of inlet and outlet conditions is negligible.

3.5.2 Mean-line and Through Flow Modelling

Another technique used to predict turbine performance is the mean-line and through flow modelling techniques. Both mean-line and through flow codes use blade cascade tests to generate empirical performance curves as a function of key blade geometric parameters. Mean-line codes apply the empirical performance curves at only one streamline surface along the equivalent mean turbine radius. Through-flow codes extend mean-line tools by modifying and applying loss and performance models in the span-wise direction. Hence multiple stream surfaces are used to capture performance and loss from blade hub to tip. The advantages of using mean-line and through-flow tools are: speed, stability, minimum input data requirement, pre- and post-processing requirements, insight into turbine flow physics, and accuracy.

TurbAero, which is a through-flow code, was used to model the Olympus HP turbine. The code extends the well known Ainley-Mathieson and Dunham-Came (AMDC) mean-line loss modelling system.

Mean-line techniques conceptualise the loss mechanisms based on turbine features. The losses are attributed to blade profile, secondary air flow, blade clearance, trailing edge, supersonic expansion and shock loses and is mathematically expressed as:

$$Y = Y_P + Y_S + Y_{CL} + Y_{TE} + Y_{EX} + Y_{SH}$$

$$Y = \frac{P_{t1}^{'} - P_{t2}^{'}}{P_{t2}^{'} - P_2}$$

where:

Y_P = Profile loss coefficient

Y_S = Secondary flow loss coefficient
Y_{CL} = Blade clearance loss coefficient
Y_{TE} = Trailing edge loss coefficient
Y_{EX} = Supersonic expansion loss coefficient
Y_{SH} = Shock loss coefficient

In most cases the profile and secondary flow losses are the primary parameters driving turbine performance. The profile loss represents losses associated with the blade geometry and flow incidence. The secondary losses are associated with the interaction between the flow through the blade passage and the end wall boundary layer. Blade clearance loss accounts for the additional losses due to tip clearance in unshrouded blade rows. Trailing edge loss is treated as a classic sudden expansion loss where the effect of the blade trailing edge thickness can be significant. The supersonic expansion loss and shock loss account for shocks that occur in certain regions along the blade passage and when flow is supersonic.

3.5.3 Turbine Performance Map

The results of the CFD generated turbine performance map can be seen in Figure 10.

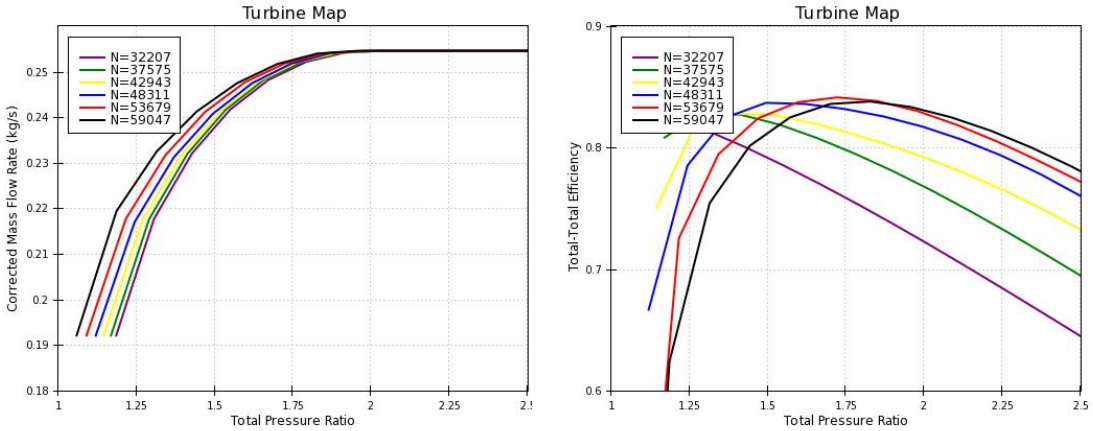

Figure 10 CFD generated turbine map

A comparison of the CFD and mean-line/through generated turbine maps can be seen in Figure 11.

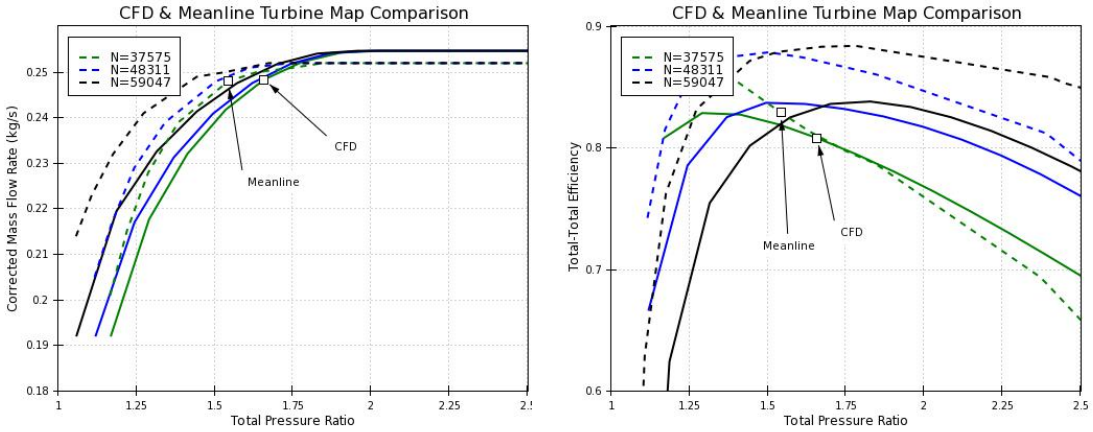

Figure 11 Comparison of CFD and mean-line/through generated turbine maps at three different speeds

From the relative mass flow rate comparison it can be seen that agreement between CFD and mean-line/through flow results is good. The mean-line/through-flow choked mass flow rate agrees to within 1% of CFD generated mass flow rate. At pressure ratios below the choking point the corrected mass flow rate for mean-line/through-flow method predicts greater corrected mass flow rate when compared to CFD. The agreement between the total-to-total efficiency results show very good agreement, however; there is a positive vertical shift in efficiency of approximately 3-5% for the mean-line/through flow results when compared to the CFD generated efficiency at high rotational speeds. The shift in the total-to-total efficiency is primarily associated to the fact that TurbAero does not apply a sudden expansion correction factor to the step change in hub and shroud radii between the turbine nozzle and rotor.

The turbine performance curve is arguably the most difficult component to experimentally map. The combustor design is not ideal and adds a large number of complications related to combustion completeness and profile. The addition of oil into the fuel and the fact that the fuel/oil mixture exiting the bearing lubrication system is diverted back to the combustor makes the measurement of turbine inlet conditions extremely difficult. Added to this complication is the limitations imposed on instrumentation due to high temperatures and poor accessibility raises a large number of issues regarding turbine map quality as measured on an engine test stand. Hence, the agreement between CFD and the mean-line/through flow solver provides a great deal of confidence with the results.

The CFD results were used as the baseline for the Olympus HP turbine map. Data smoothing was applied to the CFD results to ensure continuity when looking at the multi-dimensional turbine map from different directions.

Subsequent modelling showed that CFD generated turbine performance under-predicted choking when calibrating the engine performance model. The under-prediction of choking mass flow rate can be associated with a number of causes related to engine performance modelling, engine component design, and instrumentation and testing. Another source of

error could be related to CFD related assumptions, boundary conditions and turbulence models. CFD is a better predictor of trend-lines rather than absolute values and scaling techniques are commonly used to better approximate actual performance (while maintaining trend-line).

The final scaled turbine map along with the unscaled map for the Olympus HP engine can be seen in Figure 12. Note that a number of speed lines have been omitted for clarity.

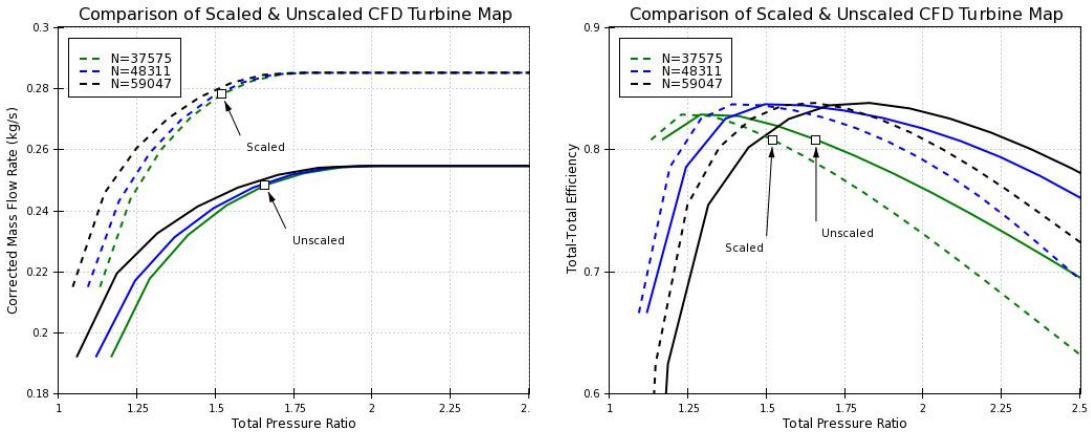

Figure 12 Olympus HP turbine performance map

3.6 Ducts

Ducts are used throughout the engine and represent the connection/transitions between components. The turbine exhaust duct is the only main duct in the Olympus HP. The combustor is also idealised as a duct for pressure loss purposes. Note that in multi-spool by-pass configurations the number of ducts increases significantly.

Adiabatic expansion is assumed in the duct which enforces conservation of enthalpy. The loss due to boundary layers and turbulence is reflected as a total pressure loss. This loss can be correlated to inlet corrected mass flow rate. The relationship is expressed as:

$$\frac{1-\frac{P_{t2}}{P_{t1}}}{\left(1-\frac{P_{t2}}{P_{t1}}\right)_{ds}} = \left(\frac{\frac{W\sqrt{RT_t}}{P_t}}{\left(\frac{W\sqrt{RT_t}}{P_t}\right)_{ds}}\right)^2$$

3.7 Nozzle

The nozzle is broken down into two sections for performance and loss modelling. The first section is the turbine exit duct.

The performance of the second part (converging section) of the nozzle is estimated using discharge and thrust coefficients to account for the effect of boundary layer and flow distortion on the nozzle exit plane. Isentropic expansion to ambient pressure is assumed. A check for sonic conditions is required. If the nozzle exit plane is found to be choked then the nozzle exit plane Mach number is set to 1.0 and static pressure calculated.

Discharge coefficient is a measure of change in effective mass flow rate to the ideal mass flow rate (assuming ideal expansion through the nozzle). It is defined as:

$$C_D = \frac{A_{eff}}{A_{geom}}$$

The main parameters affecting discharge coefficient are nozzle pressure ratio and geometric petal angle or nozzle area ratio. The nozzle discharge coefficient for the Olympus was assumed to be constant.

The effect of boundary layer and flow distortion on the gross thrust is accounted for using the thrust coefficient. The gross thrust is thrust component at the nozzle exit plane. The net thrust is the negative thrust component arising from the intake. The definition of thrust coefficient can be seen in the equation for net thrust, that is:

$$F_N = W_8 V_8 C_{FG,8} + A_8 (P_{s,8} - P_{ambient}) + W_2 V_0$$

Where 0 denotes the atmospheric free stream conditions, 2 is the engine inlet and 8 is the nozzle exit plane.

3.8 Oil/Lubrication System

The fuel flow rate is a primary parameter in engine performance modelling. The fuel/oil mixture flow rate can only be measured before it is split into two where one leads to the combustor and the other to the bearings. In order to estimate the ratio of combustor fuel flow to the lubrication fuel a test was conducted.

The test was conducted under ambient conditions where the fuel line was disassembled from the engine and fuel pumped through the piping system. The flow coming out of the combustor and lubrication line was then collected into a container. The ratio of lubrication to combustor fuel flow rate was found to be approximately 0.14.

The use of fuel flow in validation (and parameters closely linked to it) was avoided as much as possible. In instances where this was not possible, it was assumed that the combustor/lubrication fuel/oil flow ratio was constant as measured during the fuel flow test.

4. Engine Testing

4.1 Engine Test Objectives and Configurations

The main objective of testing the Olympus HP engine is to validate engine performance models. The global performance parameters such as thrust, engine inlet mass flow rate, fuel flow rate and Exhaust Gas Temperature (EGT) are the four main parameters that are of interest where engine performance modelling is concerned.

Restricting the test to the measurement of only these four parameters has a number of disadvantages. The main disadvantage is that there is no scope for model adjustment and root/cause analysis when discrepancies between the engine performance model and test data are present. The validation will only yield a positive or negative outcome. The second disadvantage is that no insight into the behaviour of the engine components will be gained. Hence, measuring component thermodynamic behaviour is also considered to be a primary objective of the engine tests.

It should also be noted that the secondary objectives of the project are to investigate thrust augmentation options and flow field characteristics for fuel flow and infrared signature studies. This also required the test to provide as much insight into the component behaviour as practically possible.

Three different test configurations were utilised to achieve the test objectives.

4.1.1 Engine Operating Line Test

The engine operating line test formed the backbone of the test program and established both global and component performance parameters. The engine, under normal operating conditions is operated from idle to maximum engine rotational speed and measurements taken at various rotational speeds. This test yields the global performance characteristics (thrust, mass flow rate etc) and also estimation of the compressor pressure ratio and efficiency as a function of corrected mass flow rate and rotational speed.

4.1.2 Reduced Nozzle Area Test

The operating characteristics of a typical turbojet under normal operational conditions are well established. The compressor operating line (established in the engine operating line test) does not significantly change even at altitude and different flight speeds. In order to get a better understanding of the compressor behaviour and performance map a second test is required to “stress” the engine so that the operating line shifts/distorts which can then be measured and mapped.

4.1.3 Nozzle Exit Flow Blockage Test

Nozzle exit flow blockage test is another test in which the engine is “stressed” to shift its operating characteristics from the nominal. A metallic plug in the shape of a dome is

placed behind the nozzle. The distance between the nozzle and plug is reduced and the operating line test performance completed at each plug location.

4.2 Engine Test Facility

An engine test stand was constructed to test and measure engine global and component level performance data[8]. Figure 13 shows the engine test stand.

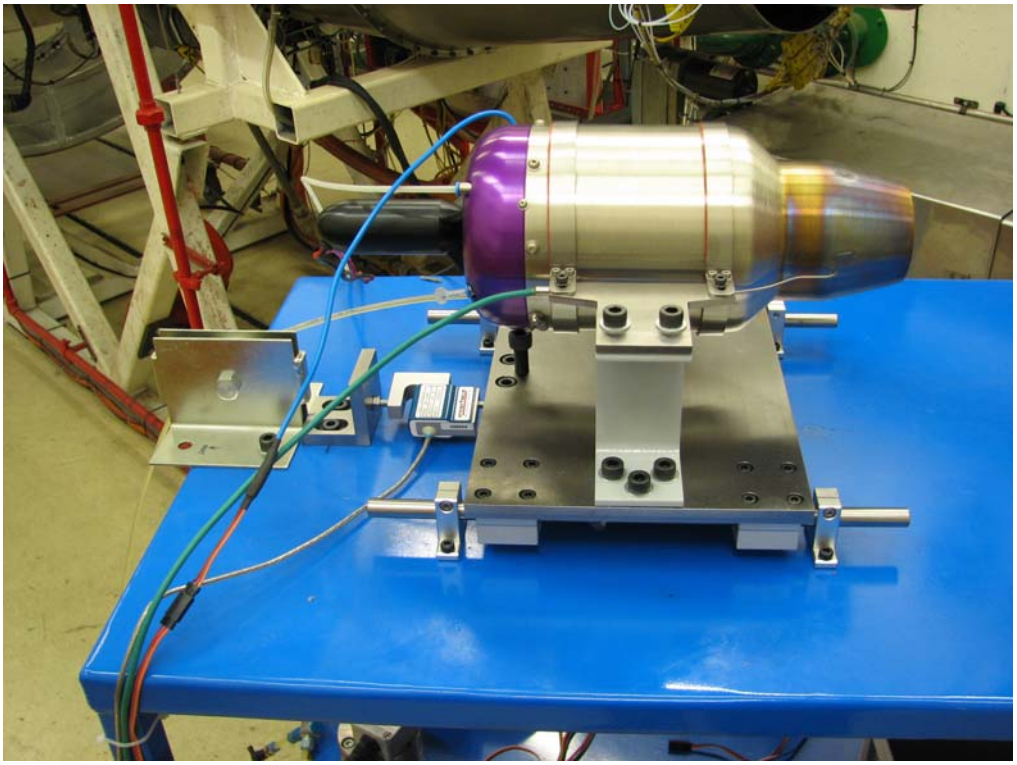

Figure 13 Engine test stand

The OEM supplied engine contained a single EGT thermocouple and a tachometer to measure engine rotation speed. The engine was subsequently instrumented with 15 static pressure tapings, 1 total pressure probe for mass flow rate measurement, 12 thermocouples to measure gas path total temperature, a load cell to measure force, fuel flow meter to measure fuel flow rate, secondary tachometer and a number of auxiliary instruments.

Engine instrumentation was selected based on detailed uncertainty analysis using both the root-mean-square and Monte-Carlo techniques. The pressure, temperature and thrust transducers were chosen to minimise the error range.

The mass flow measurement was completed using a specially design and built bell mouth which was subsequently calibrated. Details relating to the test and instrumentation design can be found in the engine test report [8].

The location and naming convention of the instruments can be seen in Figure 14.

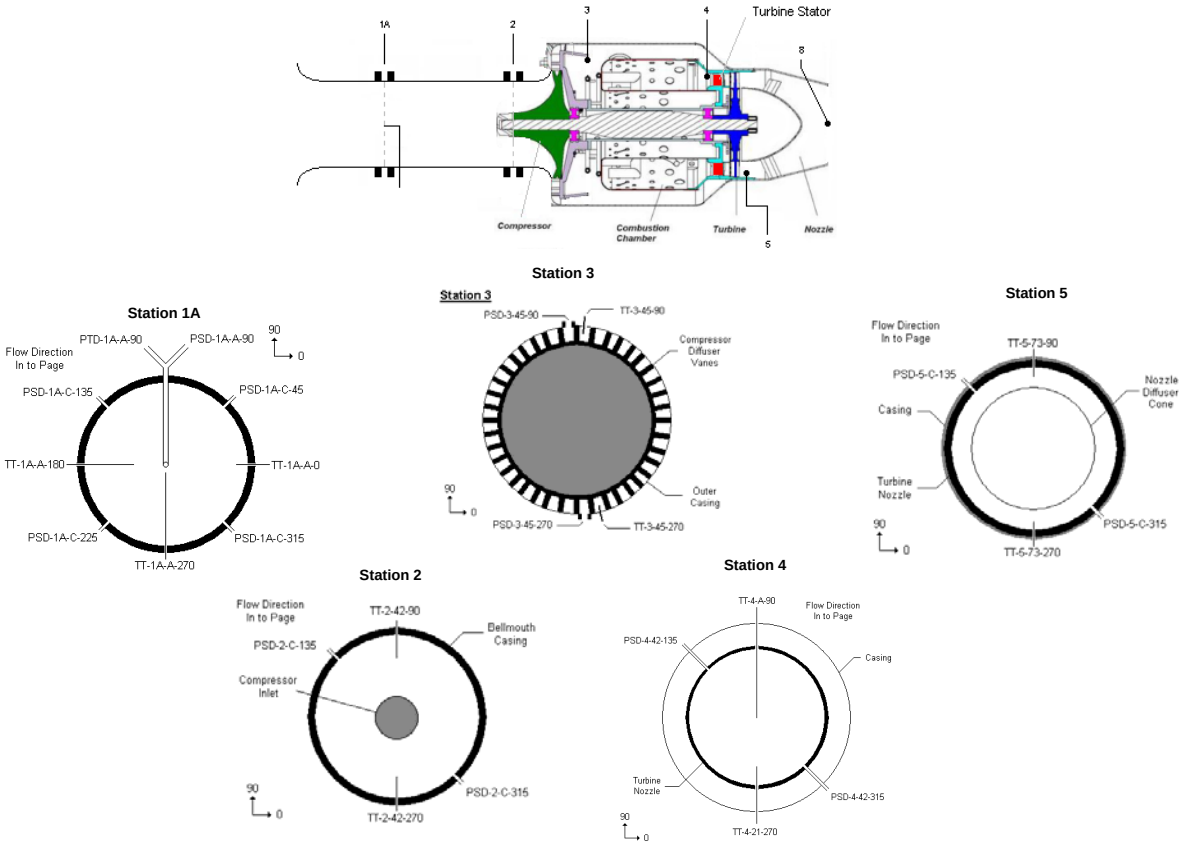

Figure 14 Engine instrumentation diagram

The test program included a reduced nozzle area test in which a conic extrusion was added to the end of the nozzle. The location of the exit thermocouple was subsequently shifted. The blockage test involved placing a conic/bullet shaped object behind the nozzle exit plane and its proximity controlled using a linear actuator mechanism.

5. Results & Discussion

5.1 Engine Operating Line

Figure 15 Comparison of the net thrust test with engine performance model and OEM data.

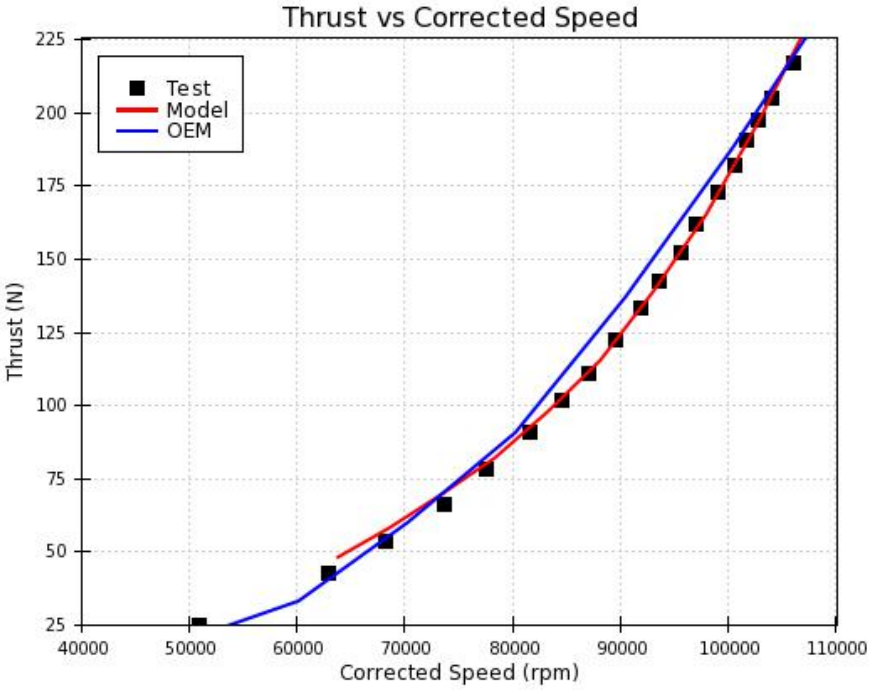

Figure 15 Comparison of the net thrust test with engine performance model and OEM data

The net thrust agreement between the engine performance model and test data is very good. The match between test data and engine performance model is better than for the data given by the OEM. The prediction quality of the model degrades slightly at rotational speeds below 75,000 rpm. This is expected as instabilities and secondary effects are usually prominent at lower speeds. It should also be noted that the area of interest in a turbojet is at high rotational speeds as this is where it will be operated during its complete flight profile (except start-up and shut-down).

A calibrated bell mouth was used to measure the mass flow rate. Figure 16 shows the mass flow rates versus engine corrected rotational speed. The performance model and test show very good agreement. The trend-line in both cases is identical. It should also be noted that the mass flow rate given by the manufacturer (0.45 kg/s at 108000 rpm) underestimates measured mass flow rate by approximately 10%.

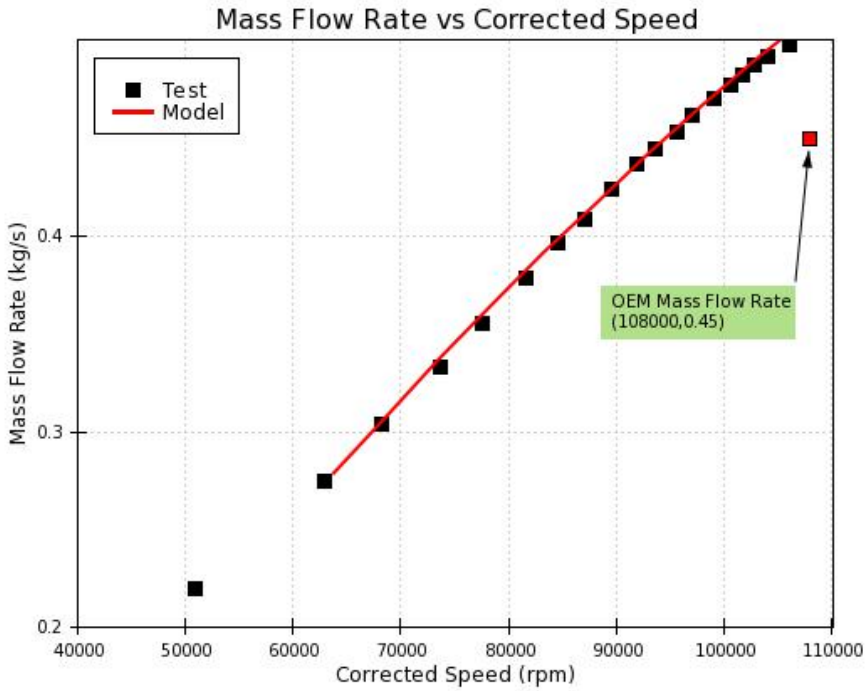

Figure 16 Fuel and air mass flow rate versus engine rotational speed

The engine fuel flow rate comparison can be seen in Figure 17. The fuel flow rate agrees well with the OEM data. The engine performance model shows a negative shift in fuel flow rate. This result is expected as the fuel flow rate given by the engine performance model refers to the fuel flow being used by the combustor. The fuel flow rate given by the OEM and measured during testing is measured at the fuel tank exit and includes the fuel diverted to the lubrication system. The fuel has been modelled using the standard JP-4 lower heating value of 43.323 kJ/kg. The inclusion of oil would effectively reduce the lower heating value which would also contribute to the shift in the engine fuel flow rate.

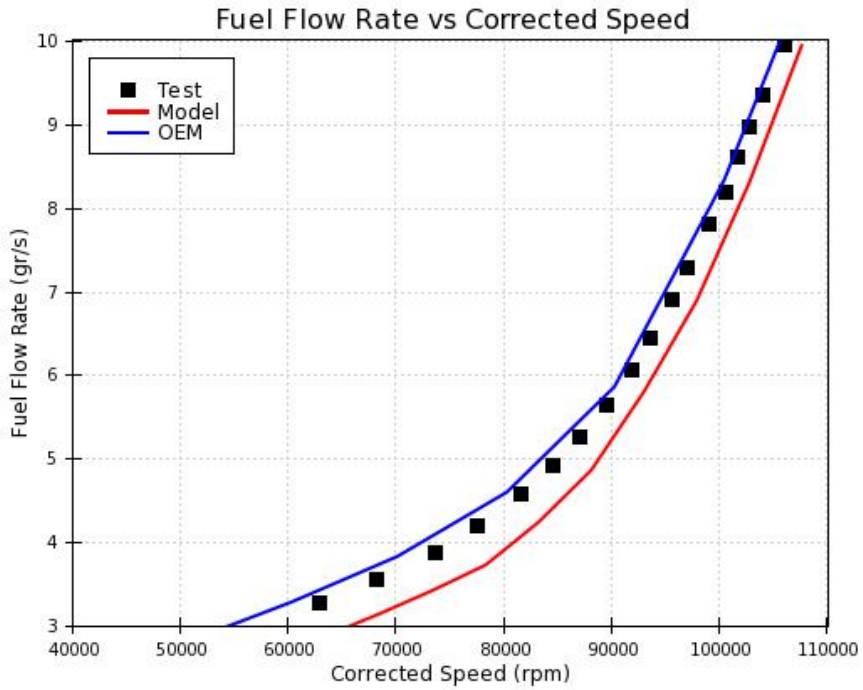

Figure 17 Fuel flow rate comparison

The exhaust gas temperature (EGT) can be seen in Figure 18. The agreement between test, OEM and performance model is good where both EGT trend-line and absolute values have been captured by the model.

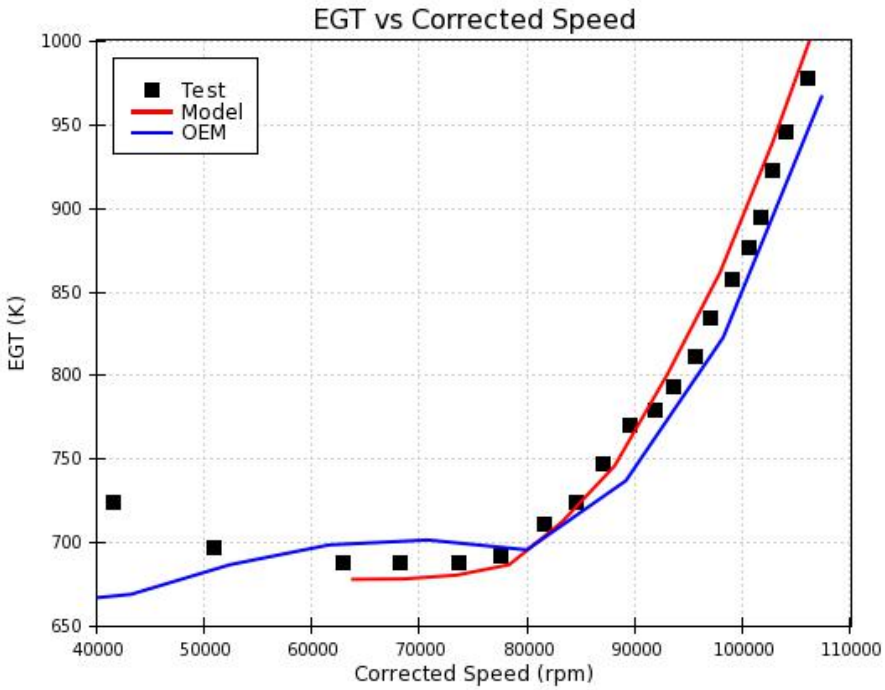

Figure 18 Exhaust gas temperature vs. corrected speed

The compressor total pressure ratio and total-total efficiencies are plotted on the compressor map in Figure 19 which also shows the engine operating line. As it can be seen from the plots the compressor model generated using the map scaling technique agrees very well with the engine behaviour.

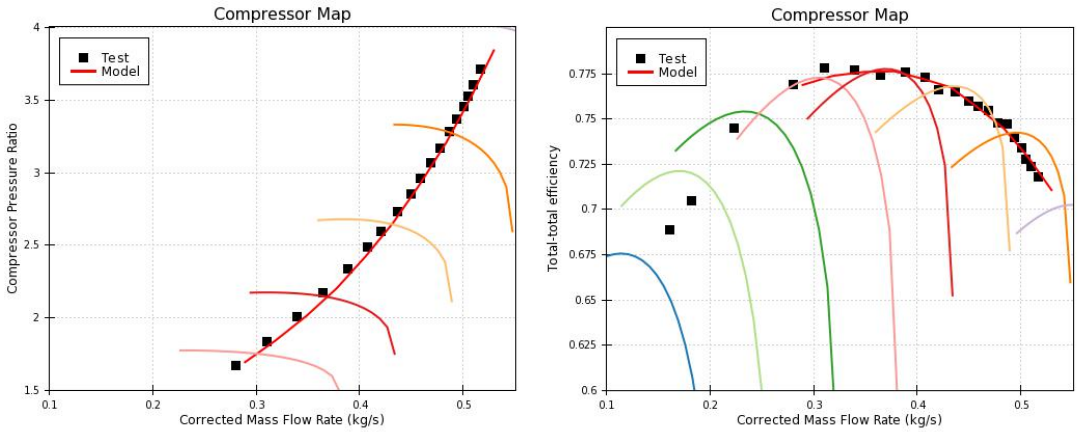

Figure 19 Compressor map and operating line

5.2 Reduced Nozzle Area

The objective of the reduced nozzle area test was to "stress" the engine and force it to operate under different operating regimes. Testing under different operating conditions would allow for better mapping of the compressor and engine performance, provide another layer of validation to the engine performance model and aid with thrust augmentation studies.

The change in thrust, mass flow rate, fuel flow rate and EGT with corrected speed and reduced nozzle area can be seen in Figure 20. The reduction in nozzle exit area increases net thrust. This is expected as the reduction in area causes the nozzle exit velocity to increase, hence increasing the momentum change between engine inlet and outlet.

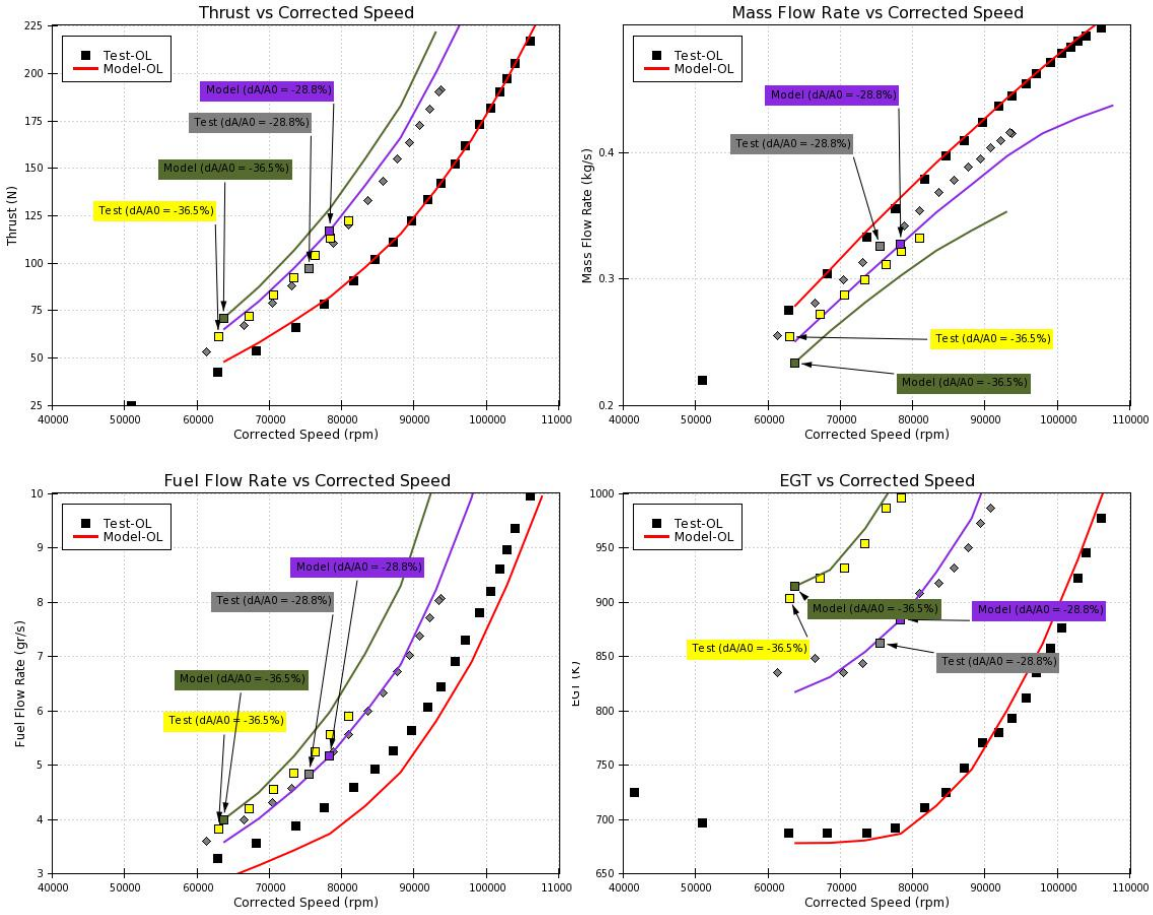

Figure 20 Change in engine performance parameters with reduced in nozzle exit area

The results show that the increase in thrust is not proportional to the change in nozzle exit area. That is, assuming identical atmospheric conditions and corrected speed, the thermodynamic state at the reduced nozzle exit plane is different. This is due to the

reduction of mass flow rate at the nozzle exit plane which causes an in-balance in the engine mass-flow rate. This in turn causes an adjustment in the engine operating conditions by shifting the compressor and engine operating line.

The vertical shift in thrust for a nozzle area reduction of 28.8% is approximately 30-50%. Note that the expected increase in thrust would be approximately 90-100% in the ideal case where the engine operating conditions did not shift. Further reduction in nozzle exit area does not significantly change thrust. This may be due to a combination of factors and the compressor reaching the stall conditions.

The agreement between test and engine performance model for the net thrust is reasonably good. In both cases the trend-line between test and model is identical. The model does over estimate the thrust in both instances. This can be associated to the compressor map and the map scaling technique used to estimate its performance. The map scaling technique starts of with a known compressor map and scales according to given data. The prediction of the compressor map boundaries and when stall and choke occur is impossible using this technique. For the purpose of this investigation the absolute values of these boundaries and the exact behaviour of the engine at regions close to stall/surge is not required, hence not pursued further.

Engine mass flow rate data also shows similar behaviour as seen for the engine thrust. The difference in this case is that the mass flow is reduced with reduced engine nozzle exit area. The trend-line correlation between test and engine performance model is also good, however the model under estimates the mass flow rate. This is also associated with the constraints on estimating the compressor map using map scaling and the accurate prediction of regions close to stall /surge and choke.

The fuel flow rate increase is substantial with the reduction in nozzle area. The increase in fuel flow (addition of energy) is required to compensate for the inefficient operating regime of the engine. The engine performance model trend-line agrees with the test data. Although it may seem that the agreement between engine performance model and test data is very good for the 28.8% nozzle area reduction test, this is not the case as the test points show total fuel flow (combustor + lubrication flow) where as the model shows the combustor fuel flow only. For a good absolute fit, a similar offset as seen in the standard operating line test would be expected.

The effects of increasing fuel flow to compensate for the in-efficiencies of the engine operating regime are clearly seen in the EGT plot. This EGT, hence turbine inlet runs at much higher temperatures in both the reduced nozzle area cases. The increase in EGT is the main limiter when conducting reduced area nozzle tests as the engine could not be operated at reasonable speeds. The increase in EGT substantially limits the use of nozzle area reduction for thrust augmentation.

The agreement between test and engine performance model for the prediction of EGT is very good. Not only is the trend-line captured but also the absolute fit is well defined.

The shift in the compressor operating line with reduced nozzle exit area can be seen in Figure 21.

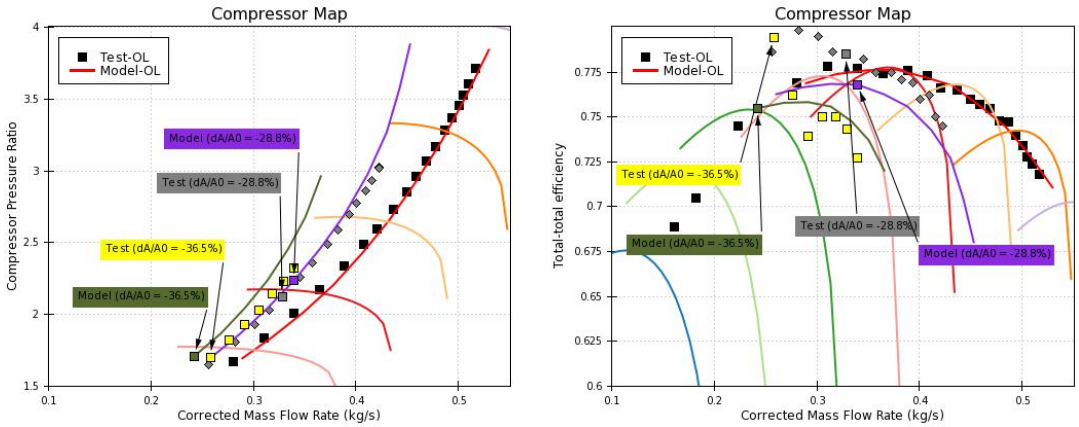

Figure 21 Change in engine compressor operating line with reduced in nozzle exit area

The operating line shifts towards the stall/surge limit as expected. The engine performance model predicts this shift reasonably well for the 28.8% area reduction case. The prediction degrades with further nozzle area reduction while maintaining good trend-line agreement. The test show that the shift is very small between the two test cases which may also suggest that the compressor might by stalled.

The compressor efficiency plot shows a large degree of scatter in efficiency when nozzle exit area is reduced. This scatter is prominent at the lower corrected mass flows (also associated with lower corrected speeds). The increase in efficiency in the lower corrected mass flow region raises a number of questions regarding the validity of the data and how well the instrumentation and processing technique is able to capture such efficiencies at or near stalled regions. The efficiencies at higher speeds/flows are reduced below the operating line case as expected. The engine performance model under predicts the change in efficiency at the higher speeds/flows.

5.3 Nozzle Exit Flow Blockage

The objective of the nozzle exit flow blockage test is the same as the reduced nozzle exit area test. It is another technique used to "stress" the engine and compressor at non-standard operating conditions to measure change in overall and compressor performance.

The test involved moving a cone/bullet shaped object towards the nozzle exit plane in increments and running an engine operating line test at each station. The cone/bullet results in a blockage to the nozzle exit air flow. This obstruction can be viewed as another loss source which the engine needs to overcome for a given condition.

Adding a blockage at the end of the nozzle results in complex flow features which can not simulated in an engine performance model without mapping the behaviour of

nozzle/blockage interaction and losses. The losses and performance penalties associated with the cone/bullet would need to be accounted for in order to obtain comparable results. Hence, it is not possible to compare the results of the nozzle exit blockage with the engine performance model.

The results for thrust, mass flow rate, fuel flow rate and EGT can be seen in Figure 22. The results mirror conclusions found in the reduced nozzle exit area test. Thrust increases with blockage due to the additional losses and energy required to overcome the blockage. The rate at which the thrust curve shifts is directly proportional to the proximity of the obstruction to the nozzle exit plane.

Mass flow rate does not change significantly for a great portion of the blockage stations. The mass flow rate drops when the cone/bullet is at 0 and -0.125 exit diameters from the nozzle exit plane. The fuel flow rate increases with the reduction in blockage as expected. The change in EGT is also significant in these tests as it was in the reduced nozzle exit area test.

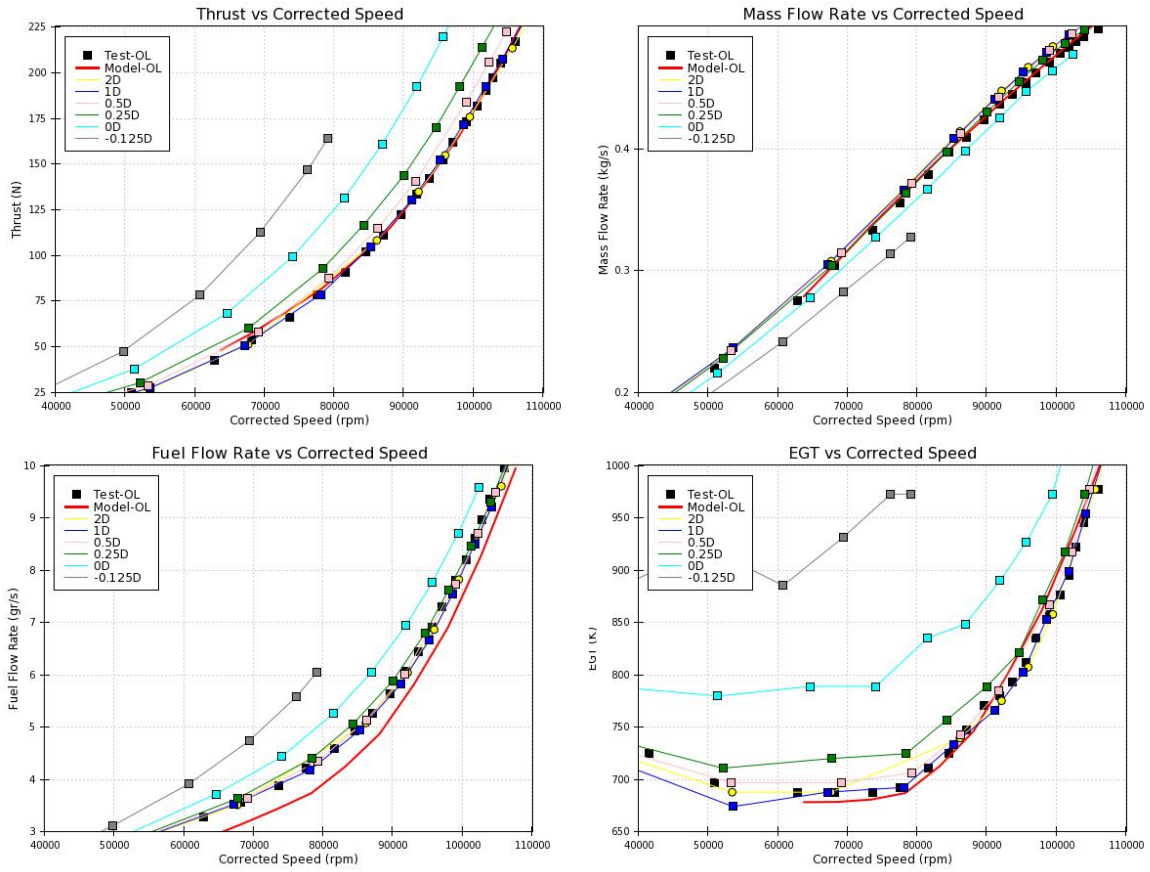

Figure 22 Change in measured engine performance parameters with nozzle exit blockage

The change in compressor operating line and efficiency can be seen in Figure 23.

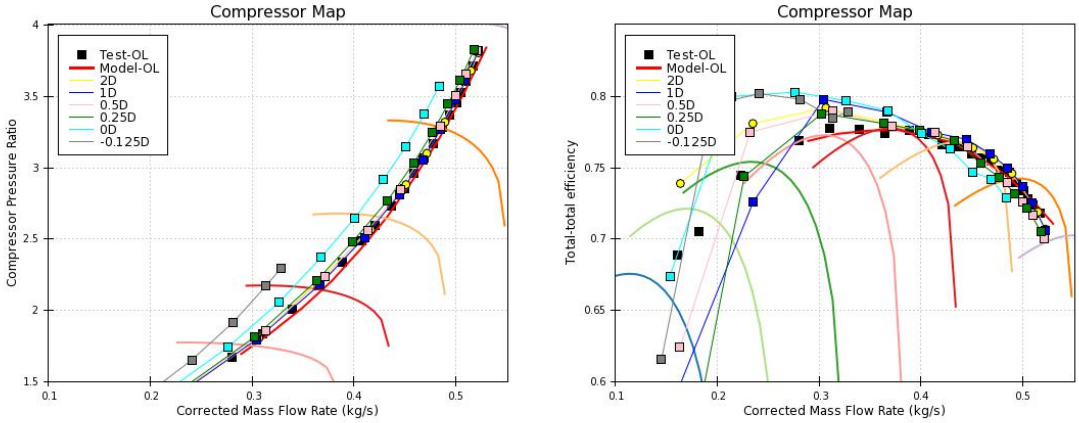

Figure 23 Change in engine compressor operating line with nozzle exit blockage

The pressure ratio plot shows the operating line shift towards the stall/surge line as expected. This shift also seems to be proportional to blockage distance from nozzle exit plane.

The efficiency plot shows little change in total-total efficiency at higher corrected mass flow rates with nozzle exit blockage distance. The scatter is also consistent with reduced nozzle area tests at lower corrected mass flow rates. There does seem to be a parabolic trend in the efficiency plot at the lower corrected mass flow rates which raise a number of issues. It could be argued that the lower corrected flow rate efficiencies are not scatter due to instrumentation and data processing but represents the actual performance of the compressor. Optimum efficiencies for the compressor would be expected at higher corrected mass flow rates and speeds which would in turn contradict this argument. This inconsistency in the results can only be answered with component testing which is beyond the scope of this project.

6. Conclusion

The primary and secondary objectives of the project were successfully completed. An in-depth analysis of engine performance modelling tools and technologies was completed. A commercial engine performance modelling tool was initially used to simulate the Olympus engine performance. An in-house code was developed and successfully bench marked against the commercial code, which was subsequently used to optimise performance parameters to improve the model output. Also, a number of tools were used in the prediction of engine component performance. The tools and techniques that were used included mean-line and through flow analysis, CFD, component map scaling, geometric data scanning and post-processing to name a few.

A comprehensive test program was successfully completed which involved the design and construction of an engine test stand. A number of components such as the engine bell-mouth, fittings and extended nozzle were designed, manufactured and installed. A large number of tests were completed using an array of instruments including standard pressure and temperature probes, traverse mechanisms and multi-holed probes.

The engine performance model agreed very well with test data. Both trend-line and absolute values matched very well at the operating line. The operating line is where the engine will work during its flight profile. The agreement of the performance parameters in "stressed" conditions was also encouraging. The trend-line was predicted accurately for all parameters with a small offset in absolute values for most of the cases. This offset was associated with the behaviour of the compressor at regions close to stall/surge and the difficulty in predicting it using the map scaling techniques.

The project also achieved its secondary objectives. A sound understanding of the engine performance was achieved and thrust augmentation options evaluated. Thrust augmentation was not pursued due to the cost and complexity in manufacturing and integrating new components into an existing engine. Infrared related CFD studies were conducted which has spurred a separate testing program to be reported subsequently. An alternate fuels project has been started which relies heavily on the knowledge and infrastructure created through this project. A final year thesis by Jones[9] has been completed and a PhD research project into infrared technologies has been started as a direct result of this program.

7. Recommendations

The project has not only helped gain an insight into engine performance modelling and testing but also raised a number of issues, obstacles and deficiencies that should be addressed in order to effectively model gas turbine engine performance.

The issues needing further investigation can be broken into two categories, namely, numerical and experimental. The following recommendations for future work can be made in the numerical simulation area:

- Although using a commercial tool for engine performance modelling provided valuable data at the early stage of the project, it also raised a large number of issues. Commercial engine performance modelling tools are mainly structured towards engine performance design. In a large number of instances this is not compatible with performance modelling of existing engines. The use of "generic maps", scaling techniques and in-built assumptions resulted in a large set of invalid performance models. Hence, it is recommended that DSTO pursue the development of its own in-house engine performance tool which can be customised for modelling existing engines based on limited data sets. An in-house

code has been developed for this project, however; it would be advisable to extend this to other engine configurations.

- The use of CFD in predicting component performance did not yield fruitful results for the compressor. A large number of CFD models were generated for the impeller and diffuser system without success. This is mainly associated with the complexity of the compressor geometry, tight spacing between impeller and radial diffuser and issues related to CFD simulation of rotating parts. The results of the turbine CFD analyses also raised a number of questions. Hence, it is advisable to start an in-depth investigation into turbo-machinery related CFD. More importantly, the project should aim to generate a set of validated process in the application of CFD to turbo-machinery. This could also form a basis for the DSTO quality management system where turbo-machinery based CFD simulations are concerned.

Experimental improvements that would greatly enhance engine performance modelling capability are:

- Enhancement of component testing facilities. The two main drivers of engine performance are the turbine and compressor. DSTO does not have a facility to characterise the aerodynamic and performance behaviour of rotating turbo-machinery components. Initially an investigation and feasibility study into a small compressor and turbine aerodynamic and performance should be completed. If feasible, a small compressor and turbine test facility would provide a very good foundation for future research into engine performance modelling and aerodynamic related issues and challenges faced by DSTO.

8. References

[1] TurbAero Software Website, http://www.turbo-aero.com/Pages/TurbAero.aspx

[2] CompAero Software Website, http://www.turbo-aero.com/Pages/TurbAero.aspx

[3] Numeca Software Website, http://www.numeca.com/

[4] GasTurb Software Website, http://www.gasturb.de/index.html

[5] "AMT Olympus HP Specifications", Advanced Micro Turbines, Netherlands, Sourced from http://www.amtjets.com/OlympusHP.php, 2009.

[6] AMT Olympus HP Operating Manual.

[7] Rahman, N, "Propulsion and Flight Controls Integration for the Blended Wing-Body Aircraft",
Cranfield University, UK, 2009.

[8] Anderson, W., "Development of the Microturbine Test Stand and Experimental Investigation of a Microturbine Engine",DSTO Technical Report, 2012.

[9] Jones, B., "Optimisation of a Small Gas Turbine Engine", Monash University, 2011.

DEFENCE SCIENCE AND TECHNOLOGY ORGANISATION
DOCUMENT CONTROL DATA

1. PRIVACY MARKING/CAVEAT (OF DOCUMENT)

2. TITLE

An Investigation into Performance Modelling of a Small Gas Turbine Engine

3. SECURITY CLASSIFICATION (FOR UNCLASSIFIED REPORTS THAT ARE LIMITED RELEASE USE (L) NEXT TO DOCUMENT CLASSIFICATION)

Document	(U)
Title	(U)
Abstract	(U)

4. AUTHOR(S)

Zafer Leylek

5. CORPORATE AUTHOR

DSTO Defence Science and Technology Organisation
506 Lorimer St
Fishermans Bend Victoria 3207 Australia

6a. DSTO NUMBER	6b. AR NUMBER	6c. TYPE OF REPORT	7. DOCUMENT DATE
DSTO-TR-2757	AR-015-427	Technical Report	October 2012

8. FILE NUMBER	9. TASK NUMBER	10. TASK SPONSOR	11. NO. OF PAGES	12. NO. OF REFERENCES
2012/1121408/1	DERP	CAVD	30	9

13. DSTO Publications Repository

http://dspace.dsto.defence.gov.au/dspace/

14. RELEASE AUTHORITY

Chief, Air Vehicles Division

15. SECONDARY RELEASE STATEMENT OF THIS DOCUMENT

Approved for public release

OVERSEAS ENQUIRIES OUTSIDE STATED LIMITATIONS SHOULD BE REFERRED THROUGH DOCUMENT EXCHANGE, PO BOX 1500, EDINBURGH, SA 5111

16. DELIBERATE ANNOUNCEMENT

No Limitations

17. CITATION IN OTHER DOCUMENTS Yes

18. DSTO RESEARCH LIBRARY THESAURUS

Gas turbine, performance modeling, engine thermodynamic cycle, turbojet

19. ABSTRACT

A small gas turbine performance modelling and testing project has been completed as part of a Divisional Enabling Research Program (DERP). The main objective of the program was to enhance DSTO's capability in understanding and modelling the thermodynamic and performance characteristics of gas turbine engines. Secondary objectives of the program included the investigation of thrust augmentation technologies and infrared suppression modelling and analysis. This report presents the results of both numerical and experimental investigation into engine performance simulation. It outlines the different tools and techniques used in modeling engine component behaviour and discusses their advantages and disadvantages. The results of two different tests designed to explore engine operating regions close to compressor stall and surge is presented.